Progress In Electromagnetics Research Letters, Vol. 100, 63–71, 2021

Numerical Assessment of Red Palm Weevil Detection Mechanism in Palm Trees Using CSRR Microwave Sensors

Mohammed M. Bait-Suwailam*

Abstract—In this paper, a numerical electromagnetic model of a low-cost detection modality for red palm weevil pests in palm trees using resonant-based microwave sensors is presented. The developed sensor is based on the complementary split-ring resonator concept. The complementary resonator is easily modelled using printed circuit board technology, where the transmission response from two ports at ends of 50 Ω-matched transmission line is recorded. The microwave sensor has been designed to work at the 2.45 GHz ISM-band and is placed underneath a finite size 3D model of a palm tree trunk infested with the red palm weevil pest. For comparison purposes, the numerical simulation results are compared against a reference case of a healthy palm trunk. The results show the capability of the proposed numerical electromagnetic model in detecting presence of the red palm weevil in palm trees.

1. INTRODUCTION

In Oman, date palm is the primary and largest agricultural crop, accounting for approximately 57% of the total cultivated area and almost 80% of all yield fruit crops. The total palm area across the Sultanate is about 36,000 hectares, with around 8,015,371 palm trees producing about 173,000 tons of dates annually [1].

Date palm trees are affected by a very serious pest, the red palm weevil (RPW), among many other pests. The number of pests that continuously attack date palms is relatively large. According to a local published survey in [2], around 24 species of insects and 3 species of mites attack date palms, among which RPWs are of major economic risks affecting the yield of date palms. Interestingly, RPW's female deposit approximately 300 eggs. Within a couple of days, eggs hatch into legless grubs that can easily penetrate into the interior of the palm trunk and then can create holes and cavities. This in turn weakens the palm tree and results in severe damage to the tree's trunk. Fig. 1 depicts the life cycle of the RPW. At start, eggs of RPW are laid on the palm tree, in cracks as well as leaf axil. Such cracks and holes are then cemented by the female RPW, thus preventing the eggs from being damaged. The life cycle of RPW from egg to adult can take from 40 to 140 days [3]. Interestingly, adult weevils live for almost 3 months feeding on palms, mating, and egg laying before dying.

The aforementioned damages caused by the red palm weevil in date palms can somehow be traced by detecting any of following symptoms: 1) low productivity of date palms, 2) palms color start to turn to yellow, 3) dryness of palm leaves, 4) presence of holes, and 5) unpleasant smell due to larvae's waste [4], as shown in Fig. 2. In fact, at an early stage of detecting any infestations, there is a high chance to get such infections cured by chemical treatments. Those undetected infestations may lead to wide spread of the RPW to neighbouring palm trees. In the worst case scenario of a severity infested palm, the injury can be seen in the area extending from the surface of the soil to about two meters high [4].

Received 3 August 2021, Accepted 1 September 2021, Scheduled 27 September 2021
* Corresponding author: Mohammed M. Bait-Suwailam (msuwailem@squ.edu.om).
The author is with the Department of Electrical and Computer Engineering, Sultan Qaboos University, Muscat, Oman.

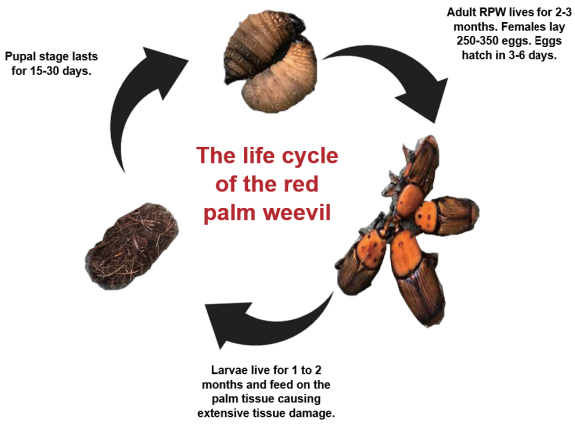

Figure 1. Schematic representation of palm weevil life cycle.

Figure 2. Snapshots taken from local real date palm garden showing several infections, larvae's waste and watery liquid.

Traditionally, there are a number of techniques that are commonly used to combat early stages of detecting RPW infestations in palm trees. Chemical treatments are a widely used procedure to disinfect palm trees from the RPW in case if other treatments fail [4]. Moreover, the deployment of RPW pheromone traps is also used, especially when the lesions appear in large quantities during date palm plantations [5]. Another method targets dead and severely infected palms by cutting them into small pieces and then burning them and thus saving other palms nearby [4].

Different methodologies for RPW pest control and management have been developed, including but not limited to the use of physical principles of X-ray radiation [6], microwave thermal heating [7–9], acoustic waves and applications of signal processing [10–12], use of infrared thermal imaging [13, 14], remote sensing imagery analysis [15, 16], and the internet of things for continuous monitoring of palm trees [17]. The use of x-ray and gamma-radiation was applied in [6] in a controlled laboratory environment. The study concluded that RPW is sensitive to incident radiation at various stages of RPW life cycle development. Microwave heating has been developed and reported by many authors using antennas for high power applications [9]. It can be inferred from many findings reported in microwave healing that treatment period of RPW adults from continuous microwave radiation at an incident power of 1 KWatt would need a minimum of 9 minutes or more depending on the insect, penetration depth and environment [9]. Recently, there has been much interest in the use of remote sensing imagery data in the detection of palm weevil. Authors in [15] studied the water stress in palm trees to aid in the detection and discrimination among different stages of red palm weevil (RPW) stress-attacks using water stress indices. Earth observation satellite imagery data were used in the study using Worldview-3 simulated data.

Recently, metamaterials have attracted lots of attention in the development of sensing and imagery microwave sensors. Microwave split-ring resonators (SRR)-based transmission lines and its complement, the complementary split-ring resonators (CSRR), have been applied to many applications, including characterization and measurement of constitutive parameters of natural materials and metamaterials, microfluidics, soil moisture contents, healthcare, to name a few [19–23]. In this research work, we develop a low-cost planar microwave sensor based on printed circuit board technology to aid in the early detection of red palm weevil. The microwave sensor is based on the concept of complementary split-ring resonator. Basically, by employing this planar sensor, we record the shift in the sensor's resonance frequency of the near-field, an indication of abnormality in the dielectric properties of the palm. This shift in the sensor's resonance frequency is due to the disturbance of the electromagnetic field upon an interaction of the sensor with other tissues.

To the best of authors knowledge, this particular numerical assessment has not been tackled previously using the developed microwave CSRR sensors. The proposed detection system is planar and compact, allowing for non-destructive testing. We believe that the proposed numerical studies will prove useful in the fabrication process of microwave CSRR-array sensors that can be scattered throughout palm trees for microwave imaging and diagnosis purposes. Numerical simulations are carried out here using the full-wave simulator of CST Microwave Studio, where a finite 3D model was constructed for the palm with and without RPW insects.

2. NUMERICAL SETUP OF THE DETECTION SYSTEM

The concept of developing microwave transmission lines with unique features was permissible in one way by using engineered materials, also known as *metamaterials* [24–28]. Metamaterials can be defined as engineered subwavelength inclusions that are tailored to achieve properties not yet readily available in nature [24]. Among the many features are narrow/wideband response, low-loss, left-handness, and compactness of the microwave based metamaterial-loaded transmission lines. Two essential building blocks contributing significantly to the design and development of such microwave transmission lines are a Split-Ring Resonator (SRR) that was proposed earlier by John Pendry in 1999 [25] and its complementary part, known as the Complementary Split-Ring Resonator (CSRR) that was proposed by Falcone et al. in 2004 [28]. The aforementioned inclusions are considered resonant particles with dimensions that are small enough as compared to the incident electromagnetic wave.

While SRR as a resonant inclusion responds to a great extent to a normal magnetic field, CSRR responds and resonates upon an excitation of a normal electric field. Thus, microwave CSRR based transmission lines behave as a bandstop LC-resonant element, where an equivalent circuit model of such a microwave sensor is shown in Fig. 3(c). As shown in Fig. 3(c), both inductance L and capacitance C account for the substrate inductance and parallel-plate capacitance, respectively, while L_{CSRR} and

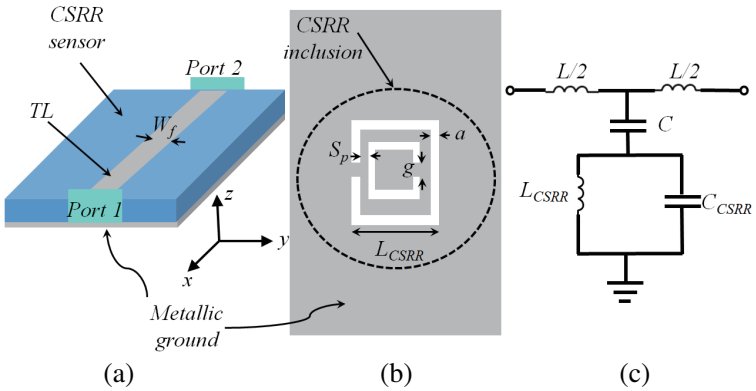

Figure 3. Schematic representation of the developed microwave CSRR sensor for RPW-infested palm detection (a) 3D view, (b) bottom view of metallic layer, and (c) the equivalent circuit model of a basic microwave transmission line loaded with CSRR inclusion. Note that gray area represents metallization.

C_{CSRR} are the inductance of rings and mutual capacitance between the rings, from which the CSRR sensor's resonance can be obtained from $1/\sqrt{(L_{CSRR}C_{CSRR})}$. Detailed analysis of quasi-approximate analytical representation of CSRR inclusions can be found in [28–30]. In this work, we consider the deployment of such CSRRs in evaluating the sensing capability of such CSRR based sensor in identifying the existence of RPW in palm trees.

Although detection of the weevil in palm trees is a complicated process and remains somehow a challenge, the developed microwave sensor herein can be considered as an alternative approach for the pre-screening of palm samples in laboratory or in the field. Thus, it provides a quick scanning modality of near-field response from the sensor in close proximity to infested palm trees. We believe that the adoption of the presented nondestructive sensor in the framework of RPW infested palm trees detection has not been fully investigated.

The microwave sensor is based on the planar complementary split-ring resonator (CSRR) concept, where two resonant concentric split rings are etched from a metallic ground plane underneath a low-loss dielectric material. Copper material is used for the conductive elements. Thus, the sensitivity of the sensor is gauged by the response from this designed CSRR unit. A two-port transmission line segment with width, W_f, was used to record the transmission coefficient response from this sensor with and without a finite sized palm trunk (both healthy and RPW-infested trunks). For convenience, the deployed dielectric material of the sensor is Rogers RO5880 laminate with $\epsilon_r = 2.2$, $\tan\delta = 0.0009$, and the sensor's dimension is $L \times W$ along the x and y directions, respectively. In principle, the microwave CSRR sensor resonates upon an excitation of an axial (normal) incident electromagnetic wave with its electric field to the CSRR plane.

Figure 3(a) depicts perspective 3D view of the developed microwave sensor, where the CSRR inclusion within the metallic ground plane is as shown in Fig. 3(b). Note that the white region within the rings in Fig. 3(b) represents the etched out copper from the metallic ground layer. Without loss of generality, square concentric rings were employed.

Figure 4 shows the electric field distribution within the bottom metallic layer, where strong electric field can be seen along the non-split rings at the resonance frequency, as a result of the notch at the resonance.

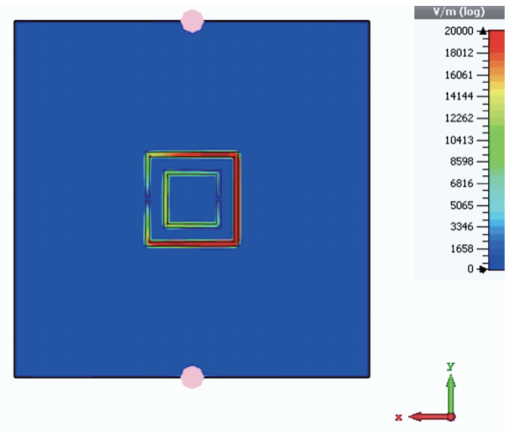

Figure 4. Electric field distribution within the CSRR resonator at the resonance frequency of 2.45 GHz.

Figure 5 shows the numerical setup of the developed microwave sensor in close proximity to a finite 3D model mimicking a palm trunk. For convenience, a 3D trunk is of cylindrical shape with a diameter D and height H, with stand off distance, S_z. The real permittivity and dielectric loss factors, $\tan\delta$, of both healthy and damaged (unhealthy) palm trunks at a frequency of 2.45 GHz are 31.5, 11.5, and 55, 9.5, respectively [18]. Note that the two modelled trunks (healthy and unhealthy trunks) were assumed to contain significant water concentration, as outlined in [18].

For comparison, a third palm trunk comprising a dry (completely damaged) palm was considered, with electrical properties as in [18]. An adult RPW was modelled here as a finite cylinder with a

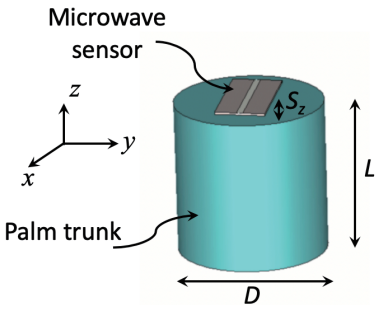

Figure 5. Numerical setup of the developed 3D microwave detection system for RPW infested palms.

diameter of 0.2 cm and height of 2.5 cm. The dielectric constant and conductivity of the RPW are set as 9.3 and 0.38 S/m as in [18]. For calibration purposes, the transmission response from the microwave CSRR sensor was numerically computed in free-space alone.

The dimensions of the optimized microwave CSRR sensor along with the 3D modeled palm trunk operating at 2.45 GHz are listed in Table 1. A relatively small 3D model of the palm trunk was considered here, due to the limited computing resources; however, that should not affect the overall performance of the proposed microwave CSRR sensor, which will be presented in next section.

Table 1. Dimensions of the optimized microwave CSRR sensor for RPW detection at the ISM band.

Parameter	Value (mm)
Length of CSRR, L_{CSRR}	10.5
Cut width, a	0.45
Gap width, g	0.5
Spacing between rings, S_p	1.575
Width of transmission line, W_f	2.52
Thickness of sensor's dielectric material	0.8
Length of substrate, L	40
Width of substrate, W	30
Diameter of palm trunk, D	50
Height of palm trunk, H	60
Stand off distance, S_z	2

3. NUMERICAL RESULTS

Figure 6 depicts the numerical simulation results for the microwave CSRR sensor alone (reference), as well as three samples of palm: healthy, infested (with highly RPW water concentration), and completely damaged dry trunks. Note that the dry trunk sample mimics a dead piece of palm, i.e., dry wood. It can be seen that the minimum transmission of the microwave CSRR sensor is at the resonance frequency of 2.45 GHz. As the CSRR sensor is placed in close proximity to the three palm trunk samples, sudden shift in the magnitude response of the transmission coefficient is observed, thus an indication of a change in the dielectric properties of the sample under test due to the change in the electric field strength as a result of waves response due to the interaction with different tissues of the three samples. Table 2 summarizes the aforementioned results, where high percentage shift in resonant frequency of the CSRR sensor is observed, which is about 5.8% for the unhealthy palm that corresponds to a deadly palm trunk, as compared to the sensor's resonance shift for the dry palm trunk, which is about 2.5%.

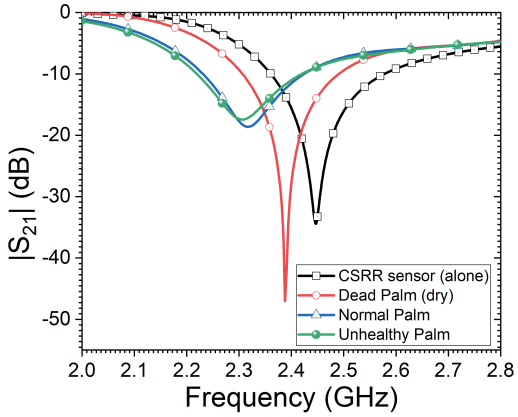

Figure 6. Numerical simulation results showing the transmission coefficient magnitude, $|S_{21}|$, for the CSRR sensor when placed in close proximity to three palm samples.

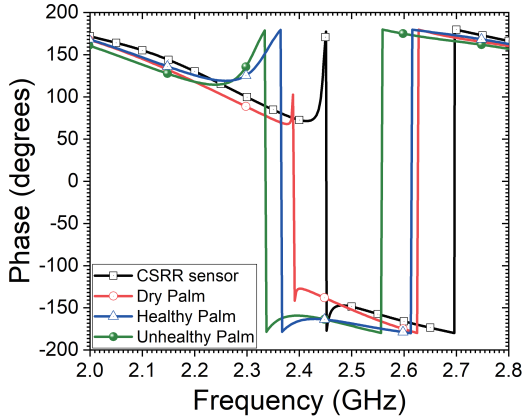

Figure 7. Numerical simulation results showing the transmission coefficient phase (in degrees) for the CSRR sensor when placed in close proximity to three palm samples.

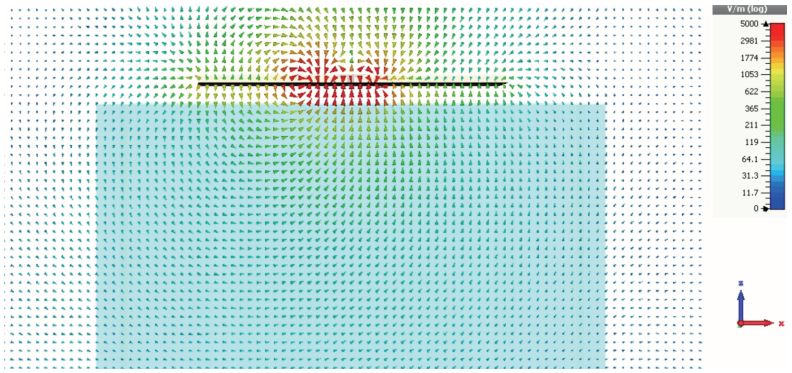

Figure 8. Electric field distribution along a lateral view for the CSRR sensor when placed in close proximity to a dry palm sample at the resonance frequency of 2.388 GHz.

Table 2. Resonant frequency of the three samples when in close proximity to CSRR sensor and the percentage shift from the resonance frequency of the reference case, i.e., CSRR alone.

Sample Type	f_{res} (GHz)	% Shift in f_{res}
Dry Palm	2.388	2.53
Healthy Palm	2.316	5.47
Unhealthy Palm	2.307	5.84

Figure 7 presents the numerical results for the phase of S_{21} for the CSRR sensor when it is brought close to three different finite palm samples and compared to the phase of the reference sensor case. As expected, there is an appreciable shift in the phase response as the sensor is brought close to the three samples, where higher shift in phase is observed for the case of unhealthy palm sample with high water concentration. Moreover, there is an abrupt change in the phase of the transmission coefficient for the case of a dry piece of palm that corresponds to a dry wood, which is attributed to the very minimal water contents in this sample compared to the other two samples.

Figure 8 depicts a snapshot of electric field distribution along the xz-plane for the CSRR microwave

sensor when it is placed in the near-zone of a dry palm sample. The E-field distribution is plotted at the resonance where the shift of the S_{21} dip was recorded, which is 2.388 GHz. As can be seen, significant E-field strength is observed with dominant normal E-field component that is supported by the transmission line quasi-TEM mode.

Table 3 summarizes several recent sensors adopted for RPW treatment compared to the proposed CSRR-based sensor. We can see that references [7, 10] focused on the use of high incident power through the sensor for heating and thus terminating existence of RPW inside palm trees, while those sensors presented in [10] and [12] used detection mean to identify potential RPW inside trees. The developed microwave CSRR sensor in this work has many features, including low-cost, planar, non-destructive testing with low power exposure.

Table 3. Comparison of recent sensors for RPW treatment with the developed microwave CSRR sensor.

Reference	Sensor basic unit cell	Sensor size	Treatment type	Fabrication cost	Nature of waves
[7]	open-ended waveguide	86×43 mm^2	heating	moderate	microwaves
[9]	vivaldi antenna	80×90 mm^2	heating	moderate	microwaves
[10]	acoustic sensor	N/A	detection	low	sound waves
[12]	optical fibers	N/A	detection	low	optical pulses
This work	planar CSRR	40×30 mm^2	detection	low	microwaves

4. CONCLUSION

In this study, a numerical analysis of 3D electromagnetic model for RPW-infested date palm detection is presented. The detection mechanism employs a near-field microwave CSRR based sensor. By recording the transmission coefficient response (either magnitude and/or phase) from the sensor when it is in close proximity to palm's tissues, it is possible to estimate any abnormality within the palm tree. Based on the numerical results, the CSRR sensor was able to detect RPW in unhealthy palm trunk sample. We believe that this microwave sensor can aid in early detection of the red palm weevil in palm trees.

ACKNOWLEDGMENT

The author would like to thank the Ministry of Higher Education, Scientific Research and Innovation for the financial support provided towards paper overlength fees.

REFERENCES

1. Al-Yahyai, R. and M. M. Khan, "Date palm status and perspective in oman," *Date Palm Genetic Resources, Cultivar Assessment, Cultivation Practices and Novel Products*, J. M. AlKhayri, S. M. Jain and D. V. Johnson, editors, Springer, the Netherlands, 2014.
2. Al-Zadjali, T., F. Abd-Allah, and H. El-Haidari, "Insect pests attacking date palms and dates in Sultanate of Oman," *Egyptian Journal of Agricultural Research*, Vol. 82, 51–59, 2006.
3. Dembilio, Ó. and J. Jacas, "Biology and management of red palm weevil," *Sustainable Pest Management in Date Palm: Current Status and Emerging Challenges*, 13–26, Wakil, Romeno Faleiro, Miller, editors, Springer, 2015.
4. El Bouhssini, M. and J. Socorro, "Date palm pests and diseases: Integrated management guide,: *International Center for Agricultural Research in the Dry Areas, (ICARDA)*, Lebanon, 2018.
5. Elmer, H. S. and J. B. Carpenter, "Pests and diseases of the date palm," *US Government Printing office, Agriculture Handbook*, No. 527, 1978.
6. Ramachandran, C. P., "Effects of gamma radiation on various stages of red palm weevil Rhynchophorus ferrugineus F," *J. Nucl. Agric. Biol.*, Vol. 20, No. 3, 218–221, 1991.

7. Massa, R., G. Panariello, D. Pinchera, et al., "Experimental and numerical evaluations on palm microwave heating for red palm weevil pest control," *Scientific Reports*, Vol. 7, 45299, 2017, doi:10.1038/srep45299.
8. Massa, R., G. Panariello, et al., "Microwave heating: A promising and eco-compatible solution to fight the spread of red palm weevil," *Arab Journal Prot.*, Vol. 37, No. 2, 134–148, 2019.
9. Rmili, H., K. Alkhalifeh, M. Zarouan, W. Zouch, and M. T. Islam, "Numerical analysis of the microwave treatment of palm trees infested with the red palm weevil pest by using a circular array of vivaldi antennas," *IEEE Access*, Vol. 8, 152342–152350, 2020.
10. Rach, M., H. Gomis, O. Granado, M. Malumbres, A. Campoy and J. Martín, "On the design of a bioacoustic sensor for the early detection of the red palm weevil," *Sensors*, Vol. 13, No. 2, 1706–1729, Jan. 2013.
11. Hussein, W., M. Hussein, and T. Becker, "Application of the signal processing technology in the detection of red palm weevil," *In the 17th European Signal Processing Conference*, 2009, 1597-1601.
12. Ashry, I., Y. Mao, et al., "Early detection of red palm weevil using distributed optical sensor," *Scientific Rep.*, Vol. 10, 3155, 2020.
13. Al-doski, J., S. B. Mansor, and H. Shafri, "Thermal imaging for pests detecting — A review," *Int. Journal Agric. For Plant*, Vol. 2, 10–30, 2016.
14. Vidal, D. and R. Pitarma, "Infrared thermography applied to tree health assessment: A review," *Agriculture*, Vol. 9, No. 156, 2019.
15. Bannari, A., A. M. A. Mohamed, and A. El-Battay, "Water stress detection as an indicator of red palm weevil attack using worldview-3 data," *2017 IEEE International Geoscience and Remote Sensing Symposium (IGARSS)*, 4000–4003, 2017.
16. Al-Megren, S., H. Kurdi, and M. Aldaood, "A multi-UAV task allocation algorithm combatting red palm weevil infestation," *Procedia Computer Science*, Vol. 141, 88–95, 2018.
17. Koubaa, A., A. Aldawood, B. Saeed, et al., "Smart palm: An IoT framework for red palm weevil early detection," *Agronomy*, Vol. 10, 987. 2020.
18. Massa, R., M. D. Migliore, G. Panariello, D. Pinchera, F. Schettino, E. Caprio, et al., "Wide band permittivity measurements of palm (Phoenix canariensis) and rhynchophorus ferrugineus (coleoptera curculionidae) for RF pest control",*J. Microw. Power Electromagn. Energy*, Vol. 48, No. 3, 158–169, 2014.
19. KT, M. S., M. A. Ansari, A. K. Jha, and M. J. Akhtar, "Design of SRR-based microwave sensor for characterization of magnetodielectric substrates," *IEEE Microwave Wireless Comp. Lett.*, Vol. 27, 524–526, 2017.
20. Soffiatti, A., Y. Max, S. G. Silva, and L. M. de Mendonça, "Microwave metamaterial-based sensor for dielectric characterization of liquids," *Sensors*, Vol. 18, 1513, 2018.
21. Alotaibi, S. A., Y. Cui, and M. M. Tentzeris, "CSRR based sensors for relative permittivity measurement with improved and uniform sensitivity throughout [0.9–10.9] GHz band," *IEEE Sensors Journal*, Vol. 20, No. 9, 4667–4678, 1 May 2020.
22. Yeo, J. and J.I. Lee, "Slot-loaded microstrip patch sensor antenna for high-sensitivity permittivity characterization," *Electronics*, Vol. 8, 502, 2019.
23. Bait-Suwailam, M. M. and I. Bahadur, "Non-invasive microwave CSRR-based sensor for diabetic foot ulcers detection," *18th International Multi-Conference on Systems, Signals and Devices (SSD)*, 1237–1240, Tunis, 2021.
24. Veselago, V. G., "The electrodynamics of substances with simultaneously negative values of ϵ and μ," *Soviet Physics Uspekhi*, Vol. 10, No. 4, 509, 1968.
25. Pendry, J. B., A. J. Holden, D. J. Robbins, and W. J. Stewart, "Magnetism from conductors and enhanced nonlinear phenomena," *IEEE Transactions on Microwave Theory and Techniques*, Vol. 47, No. 11, 2075–2084, Nov. 1999.
26. Marqués, R., F. Martín, and M. Sorolla, *Metamaterials with Negative Parameters: Theory, Design and Microwave Applications*, John Wiley & Sons, New York, USA, 2008.

27. Martín, F., "Metamaterials for wireless Communications, radiofrequency identification, and sensors (Review)", *International Scholarly Research Network, Hindawi*, 1–29, 2012.
28. Falcone, F., et al., "Effective negative-ϵ stopband microstrip lines based on complementary split ring resonators," *IEEE Microwave and Wireless Components Letters*, Vol. 14, No. 6, 280–282, 2004.
29. Baena, J. D., J. Bonache, F. Martin, et al., "Equivalent circuit models for split ring resonators and complementary split ring resonators coupled to planar transmission lines," *IEEE Trans. Microwave Theory and Techniques*, Vol. 53, 1451–1461, 2005.
30. Bait-Suwailam, M. M., L. Yousefi, and O. M. Ramahi, "Analytical models for predicting the effective permittivity of complementary metamaterial structures", *Microwave and Optical Technology Letters*, Vol. 55, No. 7, 1565–1569, July 2013.